A hysteretic absorber to mitigate vibrations of rail noise barriers

IOP Conf. Series: Journal of Physics: Conf. Series **1264** (2019) 012033 doi:10.1088/1742-6596/1264/1/012033

A hysteretic absorber to mitigate vibrations of rail noise barriers

M Basili[1*], P Casini[1], L Morelli[1] and F Vestroni[1]

[1] Department of Structural and Geotechnical Engineering, Sapienza University of Rome, Rome, Italy

[*] michela.basili@uniroma1.it

Abstract Noise barriers for high-speed train lines are subject to strong vibrations due to fluid pressure generated by moving trains. The barriers, generally made of steel cantilever beams, suffer fatigue. For their safety, it is necessary to adopt more resistant solutions or reduce their vibration, as is applied in this study. Following the fundamental work by Den Hartog on viscoelastic tuned mass dampers, later contributions on vibration mitigation have shown a variety of phenomena exhibited by a primary structure connected to a nonlinear light attachment. Vibration reduction of the structure has been observed for selected characteristics of the attachment. Here, the use of a hysteretic absorber is exploited. The device, made of light mass on rubber elements, has the advantage of directly representing the elastic and damping elements. The Bouc-Wen model describes the absorber behavior and its parameters are determined by the experimental results. Due to the dependence of the nonlinear system response on the oscillation amplitude, an optimal tuning is adjusted. The system is calibrated to behave around the 1:1 internal resonance condition. Numerical and experimental results show that the absorber effectively reduces the amplitude and the number of vibration cycles.

1. Introduction

Structures subjected to severe dynamic actions may suffer excessive vibrations. For their safety, two strategies are generally adopted, either increase their resistance or reduce the vibration intensity. Trackside structures such as noise barriers for high-speed train lines belong to structures of this kind; they are subjected to strong vibrations due to aerodynamic pressure generated by the moving train [1]. As a result, with the passage of each train, they sustain a large number of oscillation cycles and become vulnerable to fatigue. This topic is the focus of increasing attention [2-4].

In the vibration suppression field, it is common to connect the structure to be protected with an attachment, which has the role of absorbing part of the vibration energy of the excited primary structure, thus reducing vibration reduction. Different kinds of attachments, mostly nonlinear, have been proposed, with a wide variety of phenomena [5-9].

The idea of attaching a vibration absorber to the barrier columns is considered here as a possible solution for reducing vibrations. In a preliminary study, a viscoelastic tuned mass damper (VTMD) was used [10]: the attachment mass was connected to the main structure by means of a linear spring and viscous damper in parallel. In this study, a hysteretic vibration absorber (HVA), described with a Bouc-

Wen model [11, 12], is exploited and its performance is compared with those of a VTMD. The hysteretic absorber, made of a light mass on rubber elements, has the advantage of directly representing the elastic and damping components in a single element. Dynamic analyses of the two-degree-of-freedom (2DOF) system, representing the barrier and the attachment, subject to the pressure of passing trains are carried out and the results of experimental tests on the HVA are presented.

2. Noise barriers for high speed lines

Noise barriers for Italian high speed lines (HSL) are generally composed of H section steel profile columns, spaced every 3 m, constrained to the base through anchor bolts, figure 1(a). Noise panels are inserted between the profile flanges. These panels are usually made of metal (aluminum, stainless steel or galvanized steel), concrete, or transparent material (glass or PMMA), as well as a combination of same, depending on environmental aspects and costs. Experimental outcomes obtained during testing campaigns on noise barriers, evidenced their dynamic interaction with the train, which increases with the train's velocity. Specifically, these structures are highly susceptible to fatigue.

The distribution of the pressures along the barrier's height due to the passing train is not constant, reaching a maximum at the lower part, figure 1(b). This is expressed as a polynomial function of the height and depends on the train's speed, the rail-barrier distance and the interaxle spacing [1]. Whereas, by observing behavior along the longitudinal direction, it emerges that the pressure wave propagates with speed equal to that of the train. The pressure dynamic signal is characterized by two main not symmetrical impulses, corresponding to the head and tail of the train, connected by oscillations of minor amplitude, figure 1(c). The response of a column is independent of that of neighboring columns.

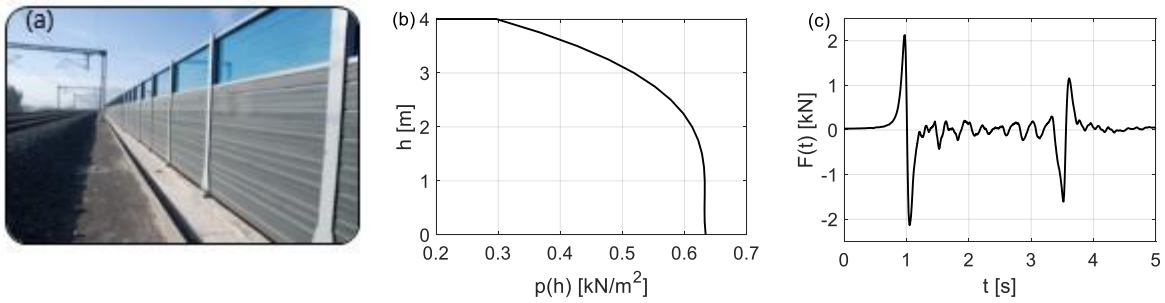

Figure 1. (a) Noise barrier in HSL, (b) hydrodynamic pressure along the barrier's height, (c) equivalent forcing action on the column. Barrier height H= 4m, train speeed 350 kph.

3. The primary structure and attachment: a 2DOF system

3.1 A SDOF model for the barrier

Columns of noise barriers are cantilever beams with distributed mass $m(x)$ and flexural rigidity $EI(x)$. Experimental tests and finite element analyses conducted on the barriers showed that the columns substantially behave in the first mode and each one deflects independently from the others [1]. For this reason, each column, with the associated part of paneling, can be studied independently and modeled as a generalized single-degree-of-freedom (SDOF) system. The deflection of the beam is a shape function $\psi(x)$ that approximates the fundamental vibration mode. The equation of motion of the generalized SDOF system, obtained by applying the principle of virtual works, is:

$$m_1\ddot{x}_1 + c_1\dot{x}_1 + k_1x_1 = F(t) \tag{1}$$

with generalized mass m_1, stiffness k_1 and force $F(t)$, defined by :

$$m_1 = \int_0^H m(x)[\psi(x)]^2\,dx \tag{2a}$$

$$k_1 = \int_0^H EI(x)[\psi''(x)]^2\,dx \tag{2b}$$

$$F(t) = g(t)\int_0^H q\,(x)\psi(x)dx \tag{2c}$$

where $g(t)$ is the normalized time history related to the passing train and its length varies with the train's speed, whereas $q(x)$ is the distributed load for unity of length applied to the column estimated as $q(x) = p(x)\cdot i$ with i interaxle spacing between two columns and $p(x)$ the pressure along the height of the barrier induced by the passage of the train, figure 1(b). The natural frequency of the SDOF system is $\omega_1 = (k_1/m_1)^{1/2}$, the damping coefficient is evaluated as $c_1 = 2\xi_1 m_1\omega_1$.
Figure 1(c) shows the force $F(t)$ applied to the generalized SDOF system for a train speed of 350 kph.

3.2 The hysteretic vibration absorber and the 2DOF system

By adding the attachment to the primary system, the 2DOF system shown in figure 2(a) is obtained. The secondary mass m_2 is connected to the primary mass by means of an element with hysteretic behavior described by the Bouc-Wen model [11, 12]. The mass ratio between the secondary and primary system is defined as $\mu = m_2/m_1$.
The equations of motion of the resulting 2DOF system are:

$$m_1\ddot{x}_1 + c_1\dot{x}_1 + k_1x_1 - f(x) = F(t) \tag{3a}$$

$$m_2\ddot{x}_2 + f(x) = 0 \tag{3b}$$

where the restoring force of the attachment is:

$$f(x) = k_2x + z(x) \tag{4}$$

having defined the relative displacement between the two masses as $x = x_2 - x_1$. The forcing action time history is reported in figure 1(c). The hysteretic part z is described by the following nonlinear differential equation:

$$\dot{z} = \{k_d - [\gamma + \beta sgn(z\dot{x})]|z|^n\}\dot{x} \tag{5}$$

where the quantities $k_2, k_d, \gamma, \beta, n$ are the constitutive parameters of the Bouc-Wen law.

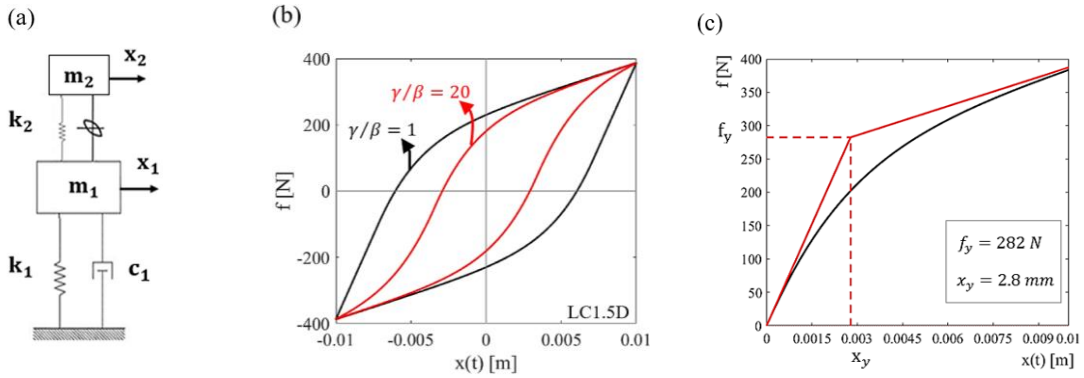

Figure 2. (a) 2DOF system, (b) Bouc-Wen model restoring force loops for γ/β =1 and 20, (c) first loading branch.

Figure 2(b) and (c) shows the constitutive law of the Bouc-Wen model: figure 2(b) shows the role of the parameters γ and β when their ratio is assumed equal or greater than one. The case of fully

hysteresis, considered here, is described by the external (black) loop with $\gamma/\beta = 1$. Figure 2(c) shows the first loading branch of the constitutive law. The evolution of the stiffness with the displacement amplitude is evident. The nominal yielding point can be observed, with force f_y and displacement x_y, defined on the bilinear curve with the same initial stiffness and the same final stiffness.

The characteristics of the hysteretic absorber attached to the primary structure are calibrated with reference to the results obtained adopting a VTMD designed according to Den Hartog's formulae [13]. Once a mass ratio μ is assumed, the optimal parameters of the VTMD, the stiffness k_0 and the damping factor ξ_0, are obtained. It is worth remarking that, for a hysteretic absorber, stiffness and damping properties depend on the displacement amplitude. This can be observed in figure 3(a) and (b), where the dependence of the secant stiffness k_e and the equivalent damping factor ξ_e with the loop amplitude *A* is shown, where ξ_e is the value of damping of a viscoelastic device which for the same amplitude dissipates the same energy of the hysteretic device. The secant stiffness decreases with amplitude, whereas the damping factor reaches a maximum at some displacement amplitudes and then decreases. Figure 3(c) portrays the frequency response curves of a SDOF system, the HVA, with a hysteretic restoring force described by equations (4) and (5) and a frequency $\omega_A = \sqrt{(k_2 + k_d)/m_2}$ for various excitation intensities. For each intensity of the harmonic force, the amplitude of the steady state oscillations is determined by numerically integrating the equations of motion of the hysteretic SDOF. The hysteretic absorber exhibits a decrease of the resonance frequency with the oscillation amplitude, according to the softening restoring force, which makes the curve of the resonance frequency bend to the left. It is well known that these curves, obtained with a fully hysteretic restoring force (black curve in Fig. 2(b)), are always stable and do not present a frequency range of coexisting solutions as those with reduced hysteresis (red curve in Fig. 2(b)), [15].

Due to these strong nonlinear characteristics, the working range of amplitudes for the hysteretic absorber must be understood. Thus it is possible to identify the expected effective stiffness and damping factor of the hysteretic element and to obtain an optimal tuning of the attachment parameters.

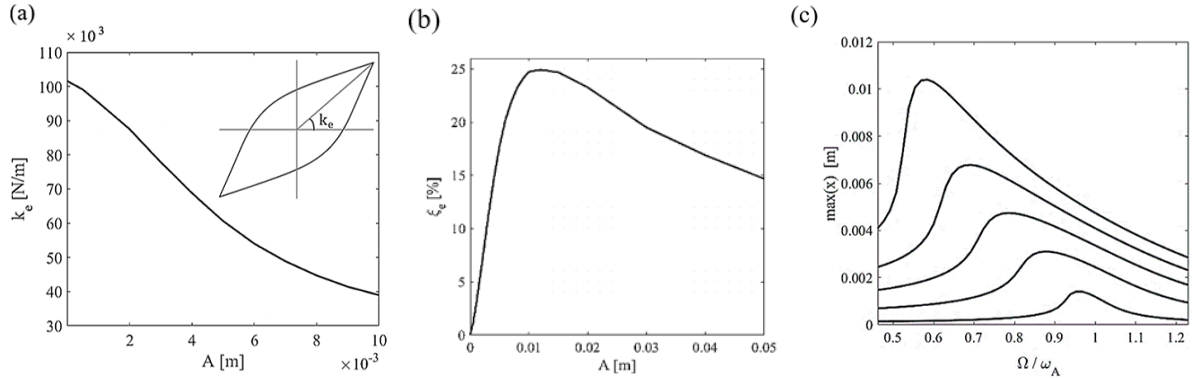

Figure 3. Bouc-Wen model, (a) the secant stiffness k_e and (b) damping factor ξ_e versus the amplitude *A*, (c) frequency response function for several amplitudes.

The main dynamic characteristics of the 2DOF system are well described by the frequency response curves (FRCs) of the primary structure subjected to a sinusoidal force, $F(t) = \Gamma f_y \sin(\Omega t)$, with driven frequency Ω and different excitation intensities, figure 4.

The optimal behavior of the VTMD, according to Den Hartog, is obtained when the frequency of the VTMD is close to that of the primary structure, figure 4(b). When dealing with a HVA, however, its frequency varies with the oscillation amplitude, therefore optimal performances of the hysteretic

absorber (figure 4(a)) are obtained only within a certain range of intensity of the excitation. Figure 3(a) shows the variation of the secant stiffness of the HVA with amplitude. For low amplitudes the stiffness k_e is greater than the optimal value k_0. The frequencies of the attachment and of the primary structure are distant and the two peaks of the FRCs are not at the same height, with the first greater than the second. At a certain intensity Γ=1.4 (red curve in the figure), the effective stiffness is close to k_0 and the amplitude of the response curve of the HVA is similar to that of the VTMD, figure 4(b). For greater amplitudes, k_e becomes lower than k_0 and the second peak becomes greater than the first, figure 4(c); as a result the HVA is not effective, due to the well-known detuning effect.

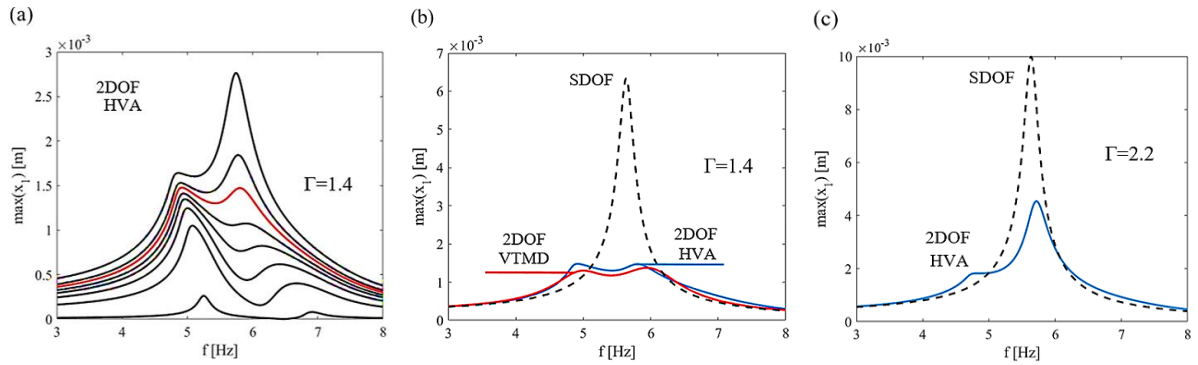

Figure 4. (a) Frequency response curves of the 2DOF system for increasing intensity, (b) comparison of SDOF and 2DOF systems responses with VTMD and optimal HVA, (c) comparison of SDOF and 2DOF systems response with HVA for large intensities.

4. Case study and numerical results

The case study refers to a 4 m high rail noise barrier, made with H section steel columns and concrete panelling. The primary structure is a cantilever beam with a 3 m wide panelling area, equal to the interaxle spacing between two columns. The damping effect is considered by assuming a damping factor of $\xi_1 = 2\%$. The total mass m_1 of the primary system is estimated considering the sum of the column and the panelling masses. The mechanical and inertial characteristics of the equivalent SDOF system is derived by equations (2) and reported in Table 1. The barrier frequency f_1=5.65 Hz is not in the zone of maximum amplification of the train forcing action, which has a maximum peak around 3 Hz, as evident in the Fourier transform reported in figure 5(a). Nevertheless, the safety of the barrier against fatigue is not satisfactory, since the structure is continuously subjected to numerous high stress cycles.

Table 1. Dynamic properties of the primary system.

m_1 [kg]	k_1 [N/m]	c_1 [N sec/m]	f_1 [Hz]
1220.7	1.5326 10^6	1730.1	5.65

A mass ratio $\mu = 0.05$ is assumed, that is the added mass m_2 is 61 kg. For the reference case of VTMD, the optimal parameters are: the stiffness k_0 =67768 N/m and the damping factor ξ_0= 0.14.

To assess the effectiveness of the absorber to mitigate the vibration of the barrier induced by train pressure, a performance index evaluated on the base of the *rms* of the response is considered:

$$i_p = \left(1 - \frac{rms(x_{1V}(t))}{rms(x_{1NA}(t))}\right)\% \tag{6}$$

where $x_{1V}(t)$ and $x_{1NA}(t)$ are the primary system displacements with the VTMD attachment and with no attachment (NA), respectively.

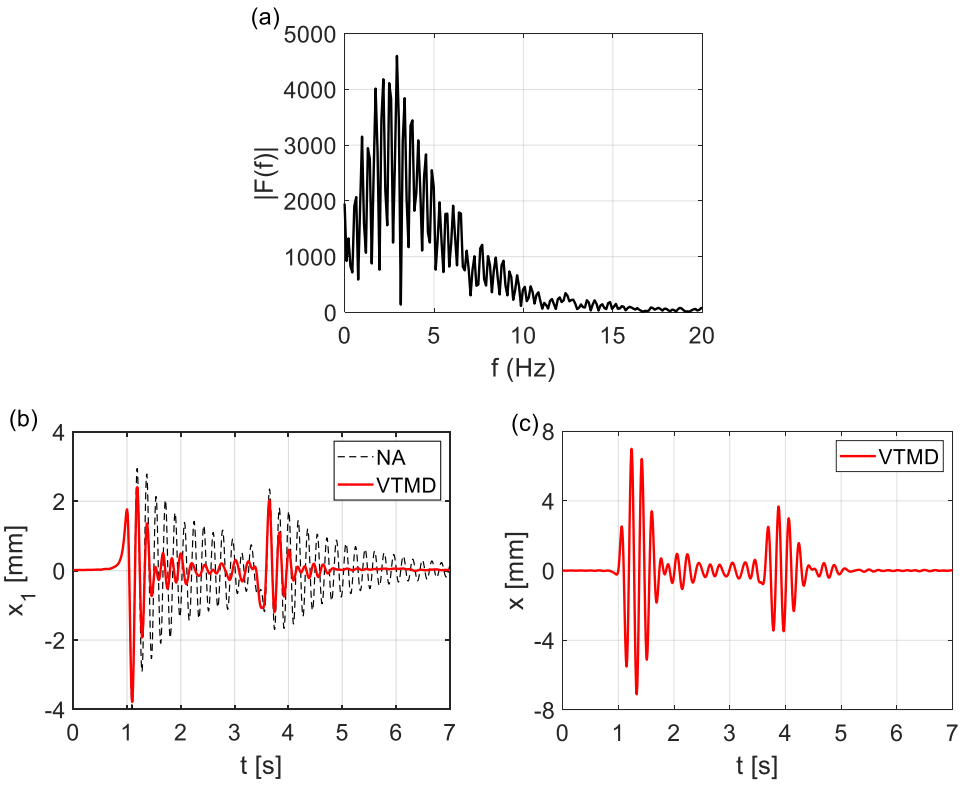

Figure 5. (a) Fourier transform of the train time history, time history of (b) the primary structure displacement with no attachment (NA) and with VTMD, (c) the relative displacement of VTMD. Train speed 350 kph.

Figure 5(b) shows the response of the barrier to the passage of the train, at a speed of 350 kph, both with the VTMD and without. The time history shows two peaks, corresponding to the head and tail of the train, with the first peak greater than the second, and lower amplitude oscillations in between. By comparing the response of system with the VTMD and without, the effectiveness of the viscoelastic device is evident. The oscillation amplitudes are strongly reduced after the two peaks; the value of the i_P index is 40%. With the VTMD the primary structure has a maximum displacement of $x_1 = 3.8$ mm, whereas the relative displacement of the device is x =7.1 mm, as observed in figure 5(c); the energy transmitted by the train to the primary structure is transferred to the VTMD.

The hysteretic absorber is designed once the 2DOF system response with VTMD is obtained. The goal is that for an oscillation of medium amplitude around 5 mm, the HVA should exhibit an effective stiffness k_e similar to the stiffness k_0 of the VTMD. To better illustrate this aspect, a numerical investigation is performed by assuming three different constitutive laws for the Bouc-Wen model with the same initial stiffness $k_A = 101600\ N/m$, and other parameters set as $\gamma = \beta = 60, \delta = k_2/k_A = 0.14$ varying the *n* parameter in order to have different yielding force f_y and yielding displacement x_y. The results are reported in Table 2 and figure 6.

Table 2. Constitutive properties of hysteretic attachments.

HVA	n	f_y [N]	x_y [m]
LC1.5B	1.09	491.5	$4.8\ 10^{-3}$
LC1.5C	1.31	180.2	$1.7\ 10^{-3}$
LC1.5D	1.20	282.4	$2.8\ 10^{-3}$

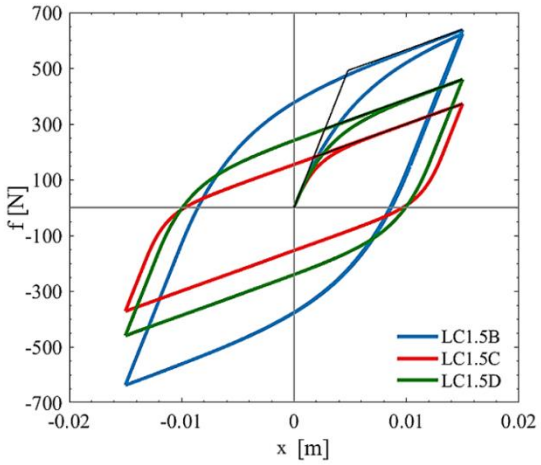

Figure 6. Hysteretic loops of HVAs.

Results of the dynamic analysis of the 2DOF system with the three constitutive relationships for the HVA show that best performances are obtained with the law LC1.5D, as can be observed in Table 3. The i_P performance index, evaluated by means of equation (6), where $x_{1V}\ (t)$ is substituted by $x_{1H}\ (t)$, the primary structure response with the added HVA, is 38%, very close to that obtained with VTMD. The adopted law is therefore LC1.5D.

Table 3. Comparison of the performance of viscoelastic and hysteretic attachments under train excitation.

$rms(x_{1NA})$ [mm]	Attachment	$rms(x_{1A})$ [mm]	i_P [%]
0.80	LC1.5B	0.50	37
	LC1.5C	0.53	34
	LC1.5D	0.49	38
	VTMD	0.47	40

Figure 7(a) shows the response of the barrier to the moving train with no attachment, the VTMD and the designed HVA attachment. By comparing the response of the primary structure equipped with the two attachments, similar results are obtained. The greatest differences are observed when the attachment has low amplitude oscillations, figure 7(b), where the effect of the detuning of the HVA can be noticed.

5. Experimental testing of the hysteretic vibration absorber

Based on the numerical results obtained in Section 4, the HVA has been attained with four high damping rubber elements and a steel plate with a 61 kg mass. Each element has a 20 mm diameter with a total 8 mm rubber thickness in order to achieve the target shear strain $\gamma_S = 100\%$, corresponding to the expected maximum displacement of the HVA. The nominal effective stiffness of each rubber element is 16000 N/m and the shear modulus of the blend is 0.4 MPa.

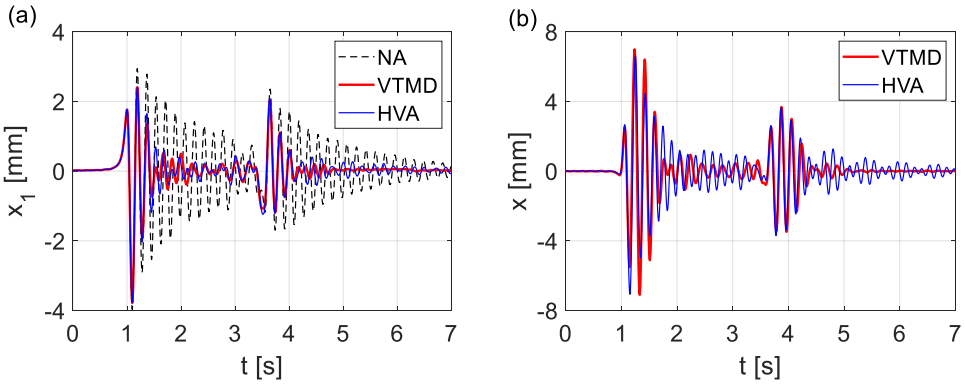

Figure 7 Time history of the (a) primary structure displacement with no attachment (NA), with VTMD and with HVA, (b) the relative displacement of VTMD and HVA. Train speed 350 kph.

Characterization tests have been conducted on each element at different values of the shear strain $\gamma_S = 25, 50, 100, 150\%$. Cyclic tests at prescribed displacement were performed using the Zwick-Roell universal testing machine at a frequency of 0.2 Hz. The machine load cell and displacement transducer were utilized to acquire the measures of force and displacement. For each test, five cycles have been made and the constitutive parameters are estimated on the third cycle. The experimental results are reported in figure 8(a). A classical identification procedure, as in [14], has been applied to determine the optimal constitutive parameters obtained by minimizing the difference between the experimental and the analytical restoring force, depending on the parameters. The identified parameters for one element are $k_2 = 10960\ N/m,\ k_d = 21750\ N/m, \gamma = \beta = 430$, whereas n has been assumed equal to one. A comparison between the experimental and identified results is shown in figure 8(b), for the exemplificative amplitude corresponding to shear strain $\gamma_S = 100\%$.

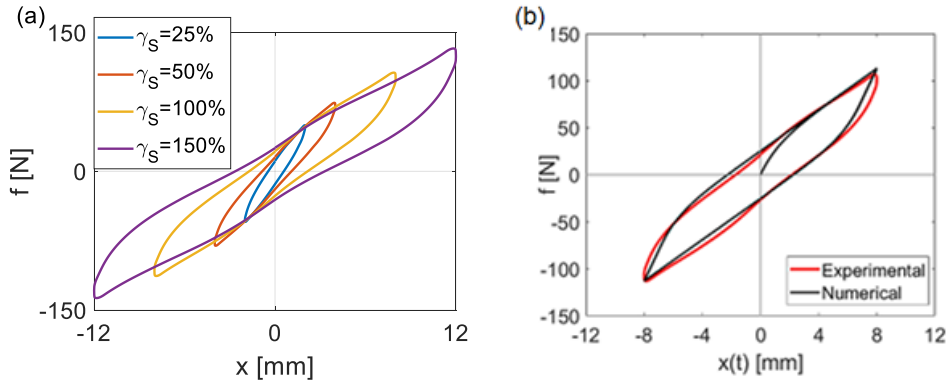

Figure 8. (a) Experimental characterization tests at different values of the shear strain γ, (b) comparison of the numerical and experimental hysteresis loops for $\gamma_S = 100\%$.

Results of the dynamic analysis of the 2DOF system with the experimentally identified law for the HVA are depicted in figures 9(a) and (b) for the primary structure and the attachment displacement, respectively, and compared with those obtained with the VTMD and NA. It can be noted that in figure 9(a) the two attachments produce a similar response of the primary structure. The i_P performance index is 38%, very close to that obtained with VTMD and analogous to the value obtained with the preliminary

designed HVA. The relative displacement between the two masses is somewhat different for the VTMD and HVA, and in particular is greater around the first peak regarding the case of HVA, figure 9(b).

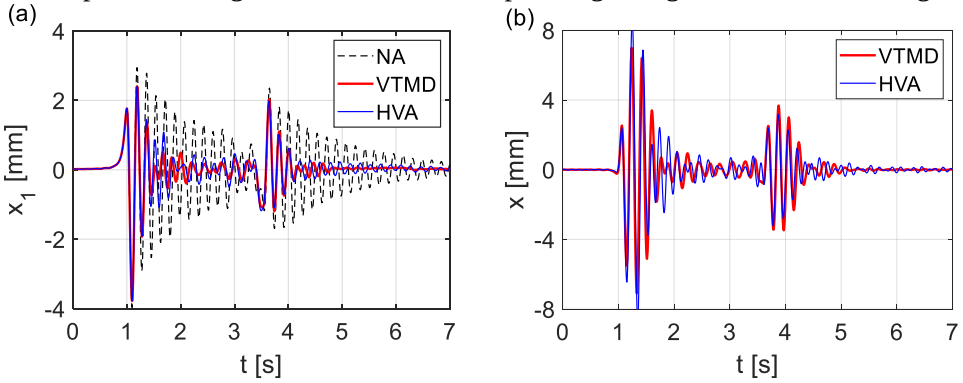

Figure 9. Time history of the (a) primary structure displacement with no attachment (NA), with VTMD and HVA experimentally identified, (b) the relative displacement of VTMD and HVA. Train speed 350 kph.

6. Conclusions

In this study a hysteretic absorber is exploited to reduce the strong vibrations produced on noise barriers of high-speed train lines due to the fluid pressure generated by the moving train. These structures are highly susceptible to fatigue due to the dynamic interaction with the moving train which increases with the speed of the train. The barrier is modelled as an equivalent SDOF system, while the hysteretic behavior of the absorber is described by the Bouc-Wen model. The design of the hysteretic absorber has been conducted on the basis of a viscoelastic tuned mass damper optimized with the theory proposed by Den Hartog. It has been shown that a variety of phenomena can be exhibited by the primary structure when the constitutive parameters of the nonlinear attachment are varied. Specifically, due to the dependence of the nonlinear system response on the oscillation amplitude, it is necessary to implement an optimal tuning of the vibration absorber.
The hysteretic device is assembled with a light mass on four rubber elements, with the advantage of directly representing the elastic and dissipative components. The Bouc-Wen parameters are identified on the basis of experimental results of characterization cyclic tests on the rubber elements. Dynamic analysis of the 2DOF system has shown the extent to which the hysteretic absorber reduces the vibration amplitude and number of cycles of the dynamic response to the train excitation. With respect to the case of no attachment, this reduction due to HVA is around the 38%, and it is similar to that obtained by using an ideal viscoelastic TMD.

Acknowledgements This work has been partially supported by the MIUR (Ministry of Education, University and Research) under the grant PRIN-2015, 2015TTJN95, P.I. Fabrizio Vestroni, “Identification and Monitoring of Complex Structural Systems”.

References

[1] Evangelista L, Vittozzi A and Silvestri G 2009 Theoretical-experimental evaluation of the noise barriers behavior on high speed lines *Ing. Ferrov.* (in Italian).

[2] Li X, Zhao Q, Zhang X and Yang D 2018 Field test and analysis of noise reduction performance

of high-speed railway semi-closed sound barriers *J. Southwest Jiaotong Univ.* **54**(4) 661-69.

[3] Xiong XH, Li AH, Liang XF and Zhang J 2018 Field study on high-speed train induced fluctuating pressure on a bridge noise barrier *J. Wind Eng. and Indust. Aerodyn.* **177** 157-66.

[4] Tokunaga M, Sogabe M, Santo T and Ono K 2016 Dynamic response evaluation of tall noise barrier on high speed railway structures *J. Sound and Vibr.* **366** 293–308.

[5] Vakakis AF 2017 Intentional utilization of strong nonlinearity in structural dynamics *Proc. Eng.* **199** 70-7.

[6] Casini P and Vestroni F 2018 Nonlinear resonances of hysteretic oscillators *Acta Mech.* **229** 939–52.

[7] Carpineto N, Lacarbonara W and Vestroni F 2013 Hysteretic tuned mass dampers for structural vibration mitigation *J. Sound and Vibr.* **333** 1302-18.

[8] Carboni B and Lacarbonara W 2016 Nonlinear dynamic characterization of a new hysteretic device: experiments and computations *Nonlin. Dyn.* **83** 23-39.

[9] Tang B, Brennan MJ, Gatti G and Ferguson NS 2016 Experimental characterization of a nonlinear vibration absorber using free vibration *J. Sound and Vibr.* **367** 159-69.

[10] Vittozzi A, Silvestri G, Genca L and Basili M 2017 Fluid dynamic interaction between train and noise barriers on High-Speed-Lines *Proc. Eng.* **199** 290-95.

[11] Bouc R 1967 Forced vibrations of mechanical systems with hysteresis *Proc. 4th Conf. Non-Linear Oscill.* Prague.

[12] Wen YK 1976 Method of random vibration of hysteretic systems ASCE *J. Eng. Mech.* **102**(2) 249-63.

[13] Den Hartog JP 1934 Mechanical Vibrations McGraw-Hill NewYork.

[14] Ni YQ, Ko JM and Wong CW 1998 Identification of non-linear hysteretic isolators from periodic vibration tests *J. Sound and Vibr.* **217** 747-56.

[15] Capecchi D and Vestroni F 1990 Periodic response of a class of hysteretic oscillators, *Int. J. Non-Linear Mechanics* **25** 309-17.